International Journal of Fatigue 155 (2022) 106626

Contents lists available at ScienceDirect

International Journal of Fatigue

journal homepage: www.elsevier.com/locate/ijfatigue

Probabilistic models for the fatigue resistance of welded steel joints subjected to constant amplitude loading

Zbigniew Mikulski *, Tom Lassen

NOV APL, Arendal, Norway
University of Agder, Grimstad, Norway

ARTICLE INFO

Keywords:
Fillet welded steel joint
High cycle fatigue
Maximum Likelihood Method
Random Fatigue Limit Model
Probabilistic resistance curves
Damage mechanisms

ABSTRACT

S-N curves found in various rules and regulations are the basic tool for the practicing engineer when carrying out life predictions for welded details in dynamically loaded structures. The present work is investigating the expected fatigue life and associated scatter for welded steel joints subjected to Constant Amplitude (CA) loading. The objective is to obtain more reliable life predictions based on advancements in the probabilistic model fitted to collected life data. A Random Fatigue Limit Model (RFLM) is proposed to obtain fatigue resistance curves at given probability levels of survival. As a distinction to more conventional statistical methods, the model is treating both the fatigue life and the fatigue limit as random variables. The focus is on high cycle fatigue and long-life data and runouts are included in a rational and logical manner by using a maximum likelihood method. Life data for a transverse fillet welded attachment originally designated as a category 71 detail in Eurocode 3 Part 1-9 are collected and analysed. The plate thickness of the specimens ranges from 20 mm to 32 mm and the steel quality is mild and medium strength Carbon-Manganese steel. The results are compared with the results obtained by conventional S-N curves. The compatibility between the fitted probabilistic models and the underlying fatigue damage mechanisms is emphasized.

1. Introduction

1.1. Design of welded details and the reliability against fatigue failure

The reliability against fatigue failure of welded details is of vital importance in the design of dynamically loaded welded steel structures. When welded joints are subjected to dynamic repetitive loading a potential fatigue failure will always be an issue of concern. Risk reduction measures must be implemented both in the detailed design of the joints and by planning of scheduled in-service inspections during the target service life. It is a major problem that the fatigue behaviour of welded joints is characterized by random variations caused by uncertainties related to residual stresses, imperfections such as the possible presence of initial flaws, and irregular weld toe geometries. These variables are often not possible to measure but they cause significant scatter in the fatigue damage evolution and final fatigue lives. Consequently, statistical analysis of life data and reliability models must be applied to handle the problem in a consistent and rational manner. Fatigue lives must be predicted at an acceptable probability of failure during the target service life for the structure. Typical examples are bridge structures, large cranes, and offshore structures.

The basic tool for engineering design is the S-N curves found in rules and recommendations. These curves are based on an exponential relationship between the applied stress range S and the number of cycles to failure N. The historical background for the development of these S-N curves has been neatly described by Murakami et al. [1] and will not be repeated herein. The curves are based on experiments with welded joints that have similar characteristics regarding the fatigue resistance. The specimens in such a test series are usually subjected to Constant Amplitude (CA) loading. This gives the necessary data for obtaining the life endurance at different stress ranges for the type of welded joint in

Abbreviations: ABS, American Bureau of Shipping; CA, Constant Amplitude; CAFL, Constant Amplitude Fatigue Limit; DNVGL, Det Norske Veritas, Germanischer Lloyd; ECCS, European Convention for Constructional Steelwork; FCAW, Flux-Cored Arc Welding; HSE, Health and Safety Executive; IIW, International Institute of Welding; LEFM, Linear Elastic Fracture Mechanics; MLM, Maximum Likelihood Method; MTTF, Mean Time to Failure; PoF, Probability of Failure; SAW, Submerged Arc Welding; SCF, Stress Concentration Factor; SIFR, Stress Intensity Factor Range; SLL, Safe Life Limit; SMAW, Shielded Metal Arc Welding; RFLM, Random Fatigue-Limit Model; TSL, Target Service Life; VA, Variable Amplitude.

* Corresponding author at: University of Agder, Jon Lilletuns vei 9, 4879 Grimstad, Norway.
E-mail address: zbigniew.mikulski@uia.no (Z. Mikulski).

https://doi.org/10.1016/j.ijfatigue.2021.106626
Received 28 July 2021; Received in revised form 27 September 2021; Accepted 21 October 2021
Available online 27 October 2021

Nomenclature

Roman letters

a	crack depth
b	fatigue strength exponent
c	crack half-length
C	crack growth rate parameter in the Paris equation
$f(t)$	frequency function
L	spacing of the weld base points
$\log a$	intercept parameter of S-N curve
m	slope parameter of S-N curve
m	crack growth rate exponent in the Paris equation
m_1	slope parameter of upper part of S-N curve
m_2	slope parameter of lower part of S-N curve
n	number of specimens
N	number of cycles to failure
N_i	number of cycles to crack initiation
$\boldsymbol{Q}$	vector containing RFLM model parameters
R	stress ratio
$R(t)$	reliability function
S	nominal stress range
t	time to failure
T	thickness of the specimen
W	width of the specimen

Greek letters

α	significance level
β_0, β_1	fatigue curve coefficients in RFLM
γ	fatigue limit defined as random variable
$\Delta\sigma$	notch stress range at the weld toe
ΔK	stress intensity factor range
ΔK_0	threshold value for the SIFR
ΔS	nominal stress range
ΔS_0	fatigue limit
$\lambda(t)$	failure rate function
$\widehat{\mu}_t$	sample mean
μ_y	mean value of the fatigue limit (logarithmic)
σ_f'	fatigue strength coefficient
σ_m	notch mean stress at the weld toe
$\widehat{\sigma}_t$	sample standard deviation
σ_y	standard deviation of the fatigue limit (logarithmic)
σ_x	standard deviation of the fatigue life (logarithmic)

question. Due to the inherent scatter in life data, both a mean curve and a characteristic curve used in design are given. The S-N curves may be based on the nominal stress range or the geometrical hot spot stress range. A more detailed overview of these topics is given by Hobbacher [2], Radaj et al. [3], Lassen et al. [4], Lotsberg [5] and Maddox [6]. Important rules and recommendations are Eurocode 3 Part 1-9 [7], HSE Offshore rules [8], DNVGL-RP-C203 [9], ABS [10] and IS0 12107 [11]. In the present work the limitations and shortcomings of this conventional statistical methodology for obtaining an S-N curve are discussed. An alternative probabilistic model based on the Random Fatigue-Limit Model (RFLM) in combination with a Maximum Likelihood Method (MLM) is investigated.

1.2. Characteristics and shortcomings of the conventional S-N curves

The present work is shortly reviewing the background and the recommended analyses for conventional bi-linear S-N curves. This is worthwhile doing because the applied methodology can still be a bit confusing for the experimentalist and the practicing engineer. The conventional procedure for establishing S-N curves for CA loading are usually characterized by:

- An elementary reliability model with the fatigue life as the single random variable is assumed to be valid at any applied stress range above what is believed to be a fatigue limit.
- The linear regression analysis carried out results in a log-normal distribution of the fatigue life because of the central-limit theorem.
- Long-lasting failures and runouts are excluded from the analysis.

The methodology is summarized in the Background Documentation 9.01a [12] for Eurocode 3 Part 1-9 [7]. Given that the fatigue damage mechanism changes as the stress range decreases it is not obvious that the same reliability model gives the best description of the scatter in fatigue life at all stress levels. It is essential to make a distinction between crack initiation and the subsequent crack growth. The distinction is important as these two phases involve different damage mechanisms. The crack initiation phase is driven by cyclic shear stress variation and the resistance against this damage mechanism is related to the yield stress of the steel. The growth phase is usually driven by the cyclic principal stresses perpendicular to the crack planes (stress mode 1) and the resistance against crack growth is not related to the yield stress, but rather to the E-modulus of the steel. Each phase must be modelled separately to capture the characteristics of the damage mechanism involved (Schijve [13]). This point of view is also supported and elaborated in the more recent work carried out by Murakami et al. [1]. The assumptions that there exists a fatigue limit may not be true. In the last proposal from IIW the fatigue limit has been rejected for the CA curves, Hobbacher [14]. IIW suggested that the lower line segment shall be given a shallow slope with a slope parameter $m = 22$ based on the work of Sonsino [15].

Furthermore, the log-normal distribution may not always be the most appropriate function for the model fitted to the life data, a competing distribution is the Weibull function, Schijve [13], Wirsching [16], Engesvik et al. [17]. Although the log-normal model is widely applied in rules and recommendation the authors have not found any formal proof that this is the best choice based on hypothesis testing. Finally, it is the present author's opinion that the long-lasting failures and runouts must not be excluded from the statistical analyses. In fact, these stress ranges are usually much closer to the magnitude of the stress ranges acting in service than the higher stress ranges applied in the linear regression for the conventional S-N curves. From that perspective the excluded data give more important information for an in-service load condition than the stress ranges that enter the linear regression analysis. Although an in-service stress spectrum gives significant additional uncertainty due to Variable Amplitude (VA) stresses the above arguments are still valid. Modification of the curve to handle VA loading must be carried out at a later stage in the same way as it is done for the conventional S-N approach. Hence, the damage accumulation under VA loading will be pursued when the life curve for CA loading has been properly understood and modelled.

1.3. The random fatigue limit model and its advantages

In the present context the expression *reliability model* is used if the model involves one random variable only such as described in the foregoing section. If several variables are involved the model shall be labelled as a *probabilistic model*. The RFLM gives a probabilistic resistance curve where both the fatigue life and the fatigue limit are treated as random variables simultaneously. The advantages of the model when compared with the conventional S-N approach are:

- The life model may change as a function of the applied stress range because of the interaction between the two random variables in the model.
- The probabilistic model can also assume any frequency function for both variables, e.g. log-normal and Weibull functions.
- An a-priori assumption regarding the existence of the fatigue limit is avoided.
- The model parameters are found based on the MLM such that long lives and runouts are included in a logical and rational manner.
- The resistance curves can be extrapolated into the very high cycle area without necessarily losing validity, although very few test results exist in this area.

1.4. Research questions and the objectives of the present work

Based on the above background the objectives and the research questions for the present work are:

1) Starting with the elementary reliability model for the finite fatigue life at a given stress range, can a conclusion be reached regarding the distribution function that gives the best fit to the life data?
2) When establishing the S-N curves with associated lower bounds based on CA life data, what are the principal differences between the conventional curves in rules and recommendations and the present resistance curve obtained by RFLM? What will be the practical outcome for fatigue life predictions based on the two approaches?
3) The focus of the present analysis will be in the high cycle regime where the RFLM includes all available data whereas the conventional S-N curves do not include these data. How is the RFLM-based resistance curve fitting these experimental data? Can any conclusion be reached regarding the existence of the fatigue endurance limit?
4) Finally, there shall be a mutual agreement between the RFLM resistance curve and the underlying damage mechanisms. Can the probabilistic curves be explained and supported by physical models for these mechanisms?

In the present study a population defined by a non-load-carrying fillet welded transverse attachment is investigated. This type of joint is designated category 71 in ENV 1993-1-9: 1992 [18] and class F in the offshore fatigue recommendations given by DNV [19]. According to current version of these standards [7,9] the proposed categorization is one level higher. The recommended categorization of such details has changed over the year, see the discussion in Section 4.3. The number that identifies the category in Eurocode 3 is defined as the fatigue strength at $N = 2 \times 10^6$ cycles. To answer research question 1 above a large amount of life data is collected at a given CA stress range of 150 MPa. The aim is to choose between the log-normal distribution and the Weibull distribution for the finite fatigue life under the same loading condition. Furthermore, a huge database at various stress ranges for the joint in question is applied to establish the conventional S-N curve and the RFLM resistance curve to answer research questions 2 and 3. In order to answer the last question 4 the underlying damage mechanisms for various phases in the fatigue damage evolution are modelled and discussed. The present work is based on the hypothesis that the understanding of the damage mechanism and which probabilistic model to select are inter-related problems.

2. Conventional S-N curves based on elementary statistical methods

2.1. Defining a population and a life model

The welded joint investigated in the present analysis is shown in Fig. 1. The applied stresses are in the main plate perpendicular to the welding direction of the transverse attachment. The multiple fatigue cracks that may appear at the weld toe are indicated with one large crack

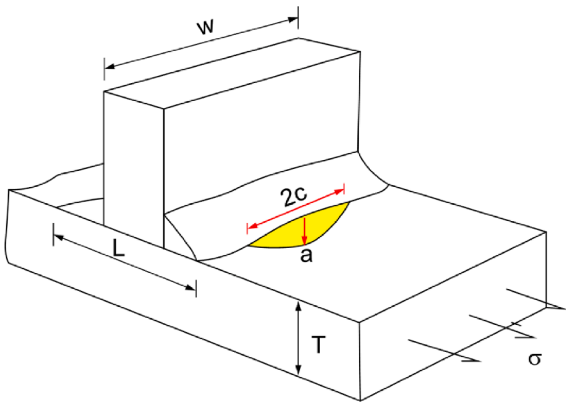

Fig. 1. Steel plate with transverse welded attachment.

only. The most important global geometry parameters with respect to fatigue are the plate thickness T and the spacing of the weld base points L. The fatigue life will increase if this distance decreases. Hence, for small attachment lengths the category changes from category 71 to category 80. The reason for this change is that the stress concentration at the weld toe decreases when the parameter L decreases. This is accounted for in Eurocode 3 Part 1-9 by a differentiation in detail category depending on the distance L when using the nominal stress range in the plate as the key to the life prediction. An alternative to this approach that circumvents this categorization problem is to use the hot spot method where the stress concentration due to the stiffener is explicitly accounted for. In the present work we shall focus on the S-N approach based on the nominal stress range. A more detailed discussion of the present category is given in Section 4.3 where the collected data are discussed. Important details for the damage evolution in the chosen welded detail is given by Mikulski and Lassen [20,21].

The consequence of the large scatter observed in test data is that the fatigue life t for a given welded joint must be treated as a random variable. For fatigue life predictions the time t is usually given in number of cycles N to failure. The associated reliability model gives the design engineer the possibility to predict the fatigue life at a chosen probability of survival. It is an advantage if enough test results are available at a given constant stress range, such that the model can be determined regarding the type of frequency function. This will also give modest statistical uncertainty for the model parameters. Unfortunately, to limit the testing efforts, the tests are usually carried out at various stress ranges with rather few tests at each stress range level. The data are then analysed directly by an S-N approach as we shall discuss in the next section. However, before pursuing the S-N approach it is important to study the behaviour of the fatigue life at a given constant stress range to understand the basic ideas of reliability modelling. In the cases where enough data are collected at a given stress range this can also give important background information for the subsequent S-N analysis at various stress range levels.

The basic characteristics for a reliability model at a given stress range are illustrated in Fig. 2. Based on the histogram fitted to the life data the frequency function $f(t)$ with associated parameters can be determined. Subsequently the reliability function $R(t)$ and the failure rate function $\lambda(t)$ are obtained. The basic mathematical equations for the model are found in Appendix A. It must be borne in mind that the reliability model shown in Fig. 2 is valid for:

- A defined damage mechanism (high cycle fatigue in the present case)
- A given quality of the welded joint (joint geometry, steel quality, welding procedures, post-weld inspections and post-weld improvement methods)
- A given operating condition (the direction of the stresses, variations of the stresses)

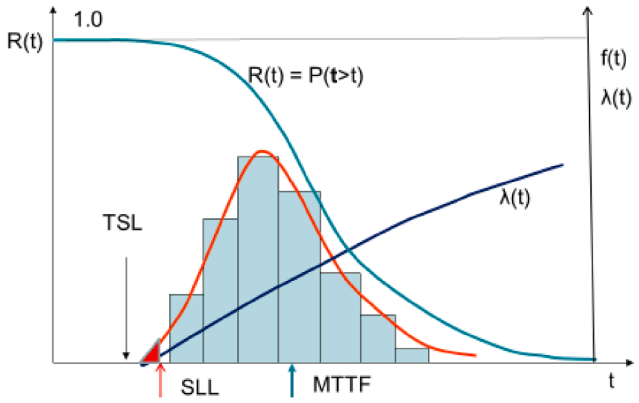

Fig. 2. Definition of a reliability model for the fatigue life.

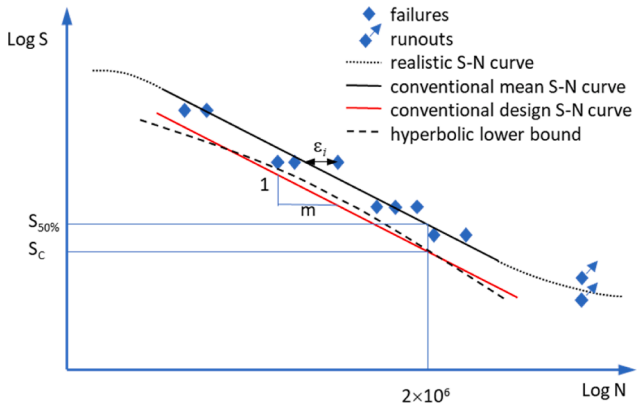

Fig. 3. An illustration of the basic concepts for the S-N curve.

The damage mechanism in the present case is high cycle fatigue, but to make things more subtle one may benefit from making a distinction between crack initiation and subsequent crack growth (Mikulski and Lassen [20,21], Lassen et al. [22]). The quality of the joint is usually given by the definition of the categories in Eurocode 3 Part 1-9. However, a category also includes considerations for the direction of the applied stresses relative to the welding direction. Finally, the given operating condition is the stress spectrum to which the welded detail is subjected during service. However, it is quite common to simplify the operating condition by applying various levels of CA stress ranges in laboratory tests. The reliability model is then conditional on an independent free variable such as the CA nominal stress range S.

In practice the design engineer must work with estimates for the true mean value μ=MTTF and the true standard deviation σ for the time to failure. These model parameters can be found by:

- The method of moments
- The least square method
- The maximum likelihood method

For a description of the two first methods the reader may look into [23]. The estimates are then generally given by a point estimate and an associated confidence interval. For the mean value the interval is determined from Student's t statistics, whereas chi-square statistics are used to determine an interval for the standard deviation. If the life data contain runouts none of the two methods are applicable. For this case a Maximum Likelihood Method (MLM) can be applied to determine the model parameters. A pioneer work for the application of the MLM for fatigue life data was carried out by Bastenaire [24].

2.2. The basic concept of an S-N curve

To obtain a life model as described in Section 2.1 at any constant stress range an S-N curve must be established. The time to fatigue failure given in number of cycles N is obtained for any CA nominal stress range S. The basic Basquin equation reads:

$$logN = loga - m{\cdot}logS + \varepsilon \tag{1}$$

The basis for this equation is shown in Fig. 3. The figure includes the data points and the fitted mean curve. In the central part of the diagram the relation between S and N is assumed linear for a log-log scale as given by Eq. (1). The fatigue damage mechanism in this area is mainly crack growth governed by the stress intensity factor range pertaining to a crack. For higher stress ranges the linear relation is overly optimistic as indicated by the dotted upper curve. This is explained by the fact that the damage mechanism changes to low cycle fatigue which is mainly governed by the plastic strain variation. For lower stress ranges the linear assumption is overly pessimistic as indicated by the dotted lower curve. Again, the explanation is related to the change in damage mechanism as the fatigue life for these low stress ranges is dominated by a crack initiation phase. Based on the data points in the mid region of the diagram a linear regression analysis is carried out for a log-log scale. The intercept parameter log a and the slope parameter m give the mean life at any stress range. A third parameter defined as the standard error is defined by the discrepancy ε for each individual data point relative to the obtained mean curve. The squared sum of the residuals will give an estimate for the standard error defining the standard deviation in the fatigue life. The standard deviation is assumed constant for all stress ranges and the design curve is found by subtracting a chosen number of standard deviations from the mean curve such that the probability of failure is regarded as acceptable. This curve is shown to the left in Fig. 3. In some cases, this design curve is chosen to be hyperbola shaped to reflect the increased confidence interval for stress ranges for which the available life data are scarce. This curve is given by the left dashed line in Fig. 3.

2.3. Some details for the conventional statistical analysis

Whereas there are no problems related to the conventional linear regression analysis, there is still some debate on how to obtain the design curves at defined probabilities of survival. Hobbacher [25,26] recommends that both the mean value and the standard deviation are chosen at an 87.5% one sided confidence level. Subsequently, these estimates are applied to determine the design curve at a 95% probability of survival. The calculations will result in a design curve that is parallel to the straight mean curve as shown by the fully drawn line in Fig. 3.

An alternative and more direct way to determine the design curve by a lower *prediction bound* is given by the equation:

$$\log N_{k,limit} = \log N_k - t_{\alpha,dof}\,\hat{\sigma}\sqrt{1+\frac{1}{n}+\frac{\left(\log S_k-\overline{\log S}\right)^2}{\sum_i\left(\log S_i-\overline{\log S}\right)^2}} \tag{2}$$

where n is the number of data points given by log S_i and log N_i which define the parameters log a and m for the mean regression line. N_k is the mean life for the considered stress range S_k. $\overline{\log S}$ is the mean of the n values of log S_i. The parameter $\hat{\sigma}^2$ is the best estimate for the variance about the regression line which is equal to the sum of squared residuals divided by the number of degrees of freedom *dof*. In the case that both the parameters log a and m have been estimated from the data, the *dof* is equal to n-2. As can be seen from Eq. (2) the Student's t-distribution still plays a central role when determining the design curve, but the chi-square distribution is no longer explicitly applied. This approach was originally based on the work by Cooper [27]. It has also been applied by Euler and Kuhlmann [28] and by Drebenstedt and Euler [29]. The shape

of the lower limit according to Eq. (2) will be a hyperbola. In the outer part of the database both the uncertainty of the mean value and the slope parameter m of the curve will be added up in life predictions. The Background Documentation 9.01a [12] uses Eq. (2) when determining the fatigue strength at 2×10^6 cycles. To facilitate the calculations the term $\log S_k$ in Eq. (2) is replaced by $\log S_{50\%}$ which is determined at $N_k = 2 \times 10^6$ cycles at the mean S-N curve. When introducing this term Eq. (2) becomes linear for a log-log scale. This linear curve is subsequently applied to define a design curve at a probability of survival chosen at 95% in the Background Documentation 9.01a. This curve is parallel to the mean curve and the characteristic fatigue strength S_C at 2×10^6 cycles can be determined. This procedure is illustrated in Fig. 3 where both $S_{50\%}$ and S_C are indicated. As can be seen the stress range S_C is slightly above the corresponding point on the hyperbola for $N = 2 \times 10^6$ cycles.

A more simplified procedure uses the line obtained in the central area of the data given in Fig. 3. This straight line is subsequently used for any applied stress range such that the hyperbola shaped curve is replaced by a straight line from the very beginning. This means that the third term under the square root in Eq. (2) is ignored. Furthermore, as the sample size increases the second term under the square root can also be neglected. This can be justified for sample sizes larger than 20. For even larger sample sizes and with a required probability of survival equal to 97.5% the value of t will approach 1.96, i.e. for $\alpha = 2.5\%$. A very informative description of these matters is given by Schneider and Maddox [30]. These simplifications are usually accepted when establishing the S-N design curves in the rules and regulations for offshore structures. This is for a limited sample size somewhat non-conservative, but this is compensated by the requirement of a high probability of survival equal to 97.5%. One may say that the offshore rules are relaxed regarding the hyperbola shape of the lower boundary line, whereas the rules are strict regarding the required survival probability level. Therefore, in these rules and regulations it has become common practice to simply subtract 1.96 standard deviations from the mean S-N curve to define the design curve.

2.4. Examples of obtained design curves for various calculation procedures

The differences in current rules and regulations regarding the type of confidence interval, how to handle the hyperbola shaped lower bound and finally the chosen probabilities of survival are summarized in Table 1.

To study the results from the two approaches recommended by the Background Documentation 9.01a and the common approach in offshore rules, the simple data sample presented by Drebenstedt and Euler [29] is applied. This data sample consists of 10 finite lives and 5 runouts, see Appendix C. Following the prescribed recommendations, the 10 finite lives were analysed by the two approaches given in Table 1. The results are given in Table 2. As can be seen the two approaches applied in civil engineering and offshore engineering give the same design curve for all practical considerations.

When determining the conventional design S-N curves for the present collected data the approach used by the offshore industry will be applied, i.e. the hyperbola shape is neglected, and the probability of survival is set to 97.5%.

Table 2
Design S-N curves based on Eurocode and the offshore recommendations.

Approach	log a (mean value)	Standard deviation	log a (design)	S at $N = 2 \times 10^6$
Eurocode 3	12.104	0.116	11.838	70.1*
Offshore rules			11.829	69.6**

*At survival probability 0.95. **At survival probability 0.975.

2.5. Assessing the conventional S-N approach in relation to involved damage mechanisms

As we have discussed the S-N curves assume that there is a single damage mechanism dominated by crack growth for any stress range. The curve is then cut off at a stress range that is designated the endurance fatigue limit. The damage mechanisms are indeed more complicated. The damage mechanism will mainly be crack growth at high stress ranges, whereas for low stress ranges the crack initiation damage mechanism will be dominant. This is in fact an objection to the basic idea of an S-N curve that assumes the same type of reliability model for any CA stress range level. Schijve [13] argued that scatter in crack initiation and crack growth are different issues. Baptista et al. [31] simulated the damage process in welded joints by three possible phases: crack initiation, micro crack growth and associated crack arrest and the final growth of larger cracks. These possible shifts in damage mechanisms explain why the long life and runout data must be excluded in the conventional analysis. These data do not obey the simple reliability model assumed to be valid for the relatively high stress range levels. This gives doubt with respect to the general validity of the S-N curves when extrapolating them down to lower stress ranges. This is also the reason why the present authors advocate the application of a RFLM as an alternative to the conventional S-N curves.

3. Resistance curves based on the random fatigue limit model (RFLM)

3.1. Basic theory and numerical procedure

The present work is based on the RFLM approach as presented by Pascual and Meeker [32]. The methodology was first applied for welded joints by Lassen et al. [33]. Similar analyses have also been carried out by D'Angelo and Nussbaumer [34] that included a Monte Carlo simulation based on the model. Toasa and Ummenhofer [35] applied a modified approach based on a general formulation of the probability weighted moments using the three-parameter Weibull distribution. This work was further developed by the authors in [36] where the focus was on how to include the result from retesting of former runouts. Leonetti et al. [37] used the RFLM for welded cover plates on girders. The work suggested to introduce more parameters to the RFLM to enhance the model fitting. Furthermore, the possibility of applying Bayesian interference is emphasized.

Table 1
Characteristics for the fatigue design S-N curves in civil engineering and offshore structures.

Rules	Application area	Type of lower bound	Hyperbolic lower bound line	Chosen probability level of survival
Background Documentation 9.01a	Civil engineering	Prediction limit	Yes	0.95
ABS	Ship and Offshore structures	Prediction limit	No	0.975
HSE				
DNVGL-RP-C203				

The basic equation of the RFLM curve reads:

$$\ln N = \beta_0 - \beta_1 ln(\Delta S - \gamma) + \varepsilon \quad (3)$$

where $\gamma = \Delta S_0$ is the fatigue-limit defined a random variable. The parameters β_0 and β_1 are fatigue curve coefficients. As can be seen, Eq. (3) s fundamentally different from Eq. (1). The life data are transformed by x = ln(ΔS) and w = ln(N). For a sample of data for x_i and w_i obtained from various test specimens $i = 1,n$, the model parameters can be determined by the Maximum Likelihood (ML) function:

$$L(\boldsymbol{Q}) = \prod_{i=1}^{n} [f_w(w_i; x_i \boldsymbol{Q}]^{\delta_i} [1 - F_W(w_i; x_i \boldsymbol{Q})]^{1-\delta_i} \quad (4)$$

where $\delta_I = 1$ if w_i is a failure and $\delta_I = 0$ if w_i is a censored observation (runout).

The vector $\boldsymbol{Q}$ contains the model parameters:

$$Q = (\beta_0, \beta_1, \sigma_x, \mu_v, \sigma_v,) \quad (5)$$

Once these parameters have been determined from optimization of Eq. (4), the corresponding confidence intervals can be obtained by a profile likelihood method using the profile ratio of the variables together with chi-square statistics. The basic equations are given in Appendix B and further details for these calculations can be found in Pascual and Meeker [32]. The optimization of Eq. (4) and the necessary integration of the involved functions must be done numerically. The problem with local maxima may occur. In the present work an algorithm is developed in Matlab to obtain the global maximum of the object function with high accuracy. For that purpose, a multivariable object function is defined based on Eq. (4). Numerically this is carried out by searching for the minimum of the function -log($L(\boldsymbol{Q})$). This nonlinear optimization problem is solved using the *fmincon* built-in function in Matlab. This is a gradient-based method dependent on the specified initial point. Hence, the global maximum is found using semi-manual procedure by comparing results for many different sets of initial values. When the parameters are determined we can calculate the fatigue life for a chosen probability p of failure, see Eq. (B4) in Appendix B. Hence, the median curve and percentile curves for design purpose are obtained.

3.2. Illustrating example

To illustrate the differences between the conventional S-N curves and the present RFLM resistance curves the data given by Drebenstedt and Euler [29] (see Appendix C and Table 2) are plotted in Fig. 4 together with the two types of curves. As can be seen the curves from the two models are quite close in the upper left region of the diagram. The RFLM curve does not deviate much from a linear line and may be approximated by a straight line if the number of finite life data increases. In the lower region the conventional curve is still linear until it stops at $N = 5 \times 10^6$ or 10^7 cycles where it is assumed to change to a horizontal line (not shown). This is in accordance with the Background Documentation 9.01a [12]. In this region of the diagram the RFLM curve captures the influence of the runouts. The fact that these test specimens could have lasted even longer gives a RFLM curve that changes slope gradually such that predicted lives will be longer. The mean RFLM curve is significantly more optimistic than the conventional curve because of the 5 runouts that are included in the sample. These runouts represent 1/3 of the entire sample of 15 specimens. Nevertheless, the RFLM design curve at a PoF of 2.5% is on the safe side of all the failures. It is seen from Fig. 4 that the RFLM-based curve does not become horizontal in the area where the fatigue limit is assumed to exist in the conventional analysis. At $N = 10^7$ cycles the RFLM curve is still falling with a shallow slope. The non-linear shape of the RFLM resistance curve is quite like the original S-N curve proposed by Weibull back in the nineteen fifties. This model was revisited by D'Antuono in a recent publication [38]. However, that model has not included a random variable for the fatigue limit and does not apply the maximum likelihood method such that runouts can be included.

4. Data analysis and choice of reliability model

4.1. Present data collection at a given constant stress range of 150 MPa

In the present section the problem of selecting an appropriate distribution for the fatigue life model at a given stress range is pursued. The issue was discussed in Section 2 and illustrated in Fig. 2. Life data are collected at a constant stress range of 150 MPa (see Table 3 and Appendix D). All results are for mild and medium strength C-Mn steel with a plate thickness of 25 and 32 mm. The typical joint configuration was shown in Fig. 1. For some of the test specimens very frequent and detailed crack depth measurements were carried out during each test. This gives a unique database containing both life data and associated crack growth histories (Mikulski and Lassen [21]). The tests were carried out at rather low R ratios. For Series 1 the effective R ratio was equal to 0.35, whereas it was 0.1 for the other test series. For further details regarding test set-up and crack growth measurements the reader may follow the references given in the right column in Table 3. A total number of 138 life data were collected for the same given stress range

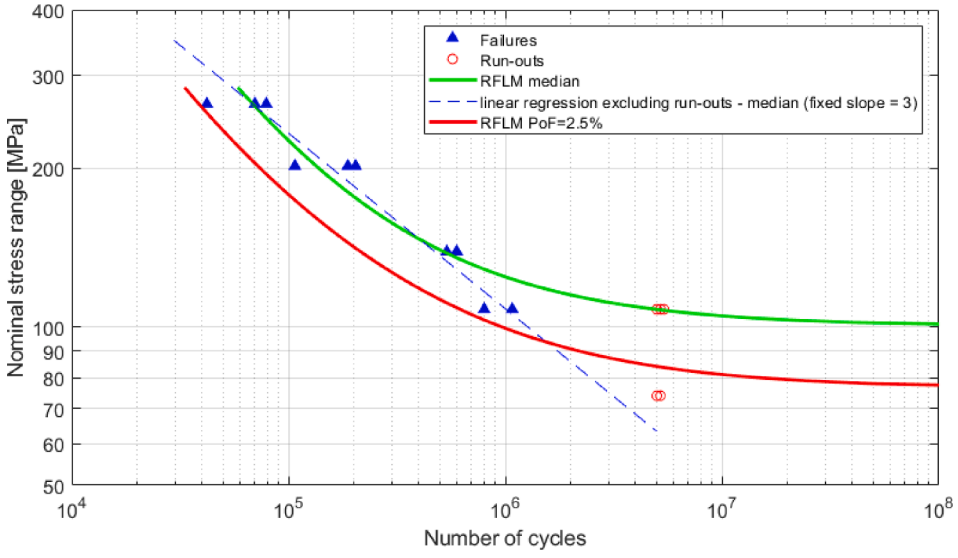

Fig. 4. S-N curves fitted to the data applied by Drebenstedt and Euler, see Appendix C.

Table 3
Overview of test series at a given applied stress range of 150 MPa.

Test data identification	Geometry	Number of specimens	Thickness	Steel grade	Welding procedure	Loading mode	Life data	Crack growth data	References
Series 1a	cruciform	34	25	S355	SMAW, FCAW	axial	x	x	1) Mikulski and Lassen [20] 2) Lassen [39]
Series 1b	cruciform	10	25	S355	SAW	axial	x	x	Lassen [39]
Series 2	cruciform	42	25	S355	SMAW	axial	x		Engesvik and Lassen [40]
Series 3	cruciform	42	32	S235	SMAW	axial	x		1) Engesvik [41] 2) Engesvik and Moan [17] 3) Engesvik and Lassen [40]
Series 4	T-joint	10	32	S355	SMAW	bending	x	x	Mikulski and Lassen [19]

and this collection permits the authors to seek the most appropriate distribution type for the life model.

4.2. Present data collection at various stress ranges

Fatigue life data at various stress ranges, besides the data presented in Section 4.1, were taken from the literature. The data collection presented in [42–44] were examined and results that were representative for the present population were included. The runout data was available only in [44]. Some fatigue life data come originally from [45–47]. These additional fatigue life data consist of 88 specimens in total, of which 15 are runouts.

4.3. Categorization and conventional life predictions for the chosen test specimen

Categorization of the welded detail in question has been changed over the years in the design standards. An overview of these changes in Eurocode 3 and DNV offshore rules is presented in Table 4. As can be seen, most of the specimens investigated in the present analysis are at the boundary given for the categorization according to the current rules. But when using the original version of these standards, the present detail has category 71 or class F undoubtedly, and this detail category is chosen in the present analysis. Moreover, the results from the present analysis of the collected life data corroborate that the chosen categorization is correct.

The following design and mean S-N curves [9] for $N < 10^7$ cycles regardless of the applied R ratio for the F class welded detail are given:

$$\begin{aligned} &\text{design}: \quad \log N = 11.855 - 3\log\Delta S \\ &\text{mean}: \quad \log N = 12.255 - 3\log\Delta S \end{aligned} \tag{6}$$

It should be mentioned that the results for test series 3 and 4 are treated as-is without any thickness correction. A minor thickness correction would not change our conclusions from the present analyses. Statistics of the total fatigue life for the entire data collection (138 specimens) are presented in Table 5. As can be seen the collected data are very close to the S-N curve statistics for an F class. The F-class mean

Table 4
Categorization of the present welded detail in the design standards.

Standard	Governing parameter	Detail category and limitation	
ENV 1993-1-9: 1992	attachment plate thickness, T	80 for $T \leq 12$ mm	71 for $T > 12$ mm
EN 1993-1-9: 2005	spacing of the weld base points, L	80 for $L \leq 50$ mm	71 for $50 < L \leq 80$ mm
DNV RP-C203 (2001)	attachment plate thickness, T	E for $T \leq 12$ mm	F for $T > 12$ mm
DNVGL RP-C203 (2016)		E for $T \leq 25$ mm	F for $T > 25$ mm

Table 5
Statistics of the total fatigue life at stress range 150 MPa.

Statistical parameter	All present test data (138 specimens)	DNVGL (F-class)
Median	455,000	533,000
Standard Deviation	278,000	288,000
Minimum	189,000	–
Maximum	2,074,000	–

S-N curve gives a median life of 533,000 cycles whereas the corresponding value from the test series is 455,000 cycles. The scatter for the present test series is given by a standard deviation of log N equal to 0.185, whereas it is close to 0.21 for the F class. Hence, the present collected test data have normal fatigue quality and are representative for the population pertaining to the F-class or category 71 in the codes.

4.4. Determining the distribution type for the life model at a stress range of 150 MPa

Before determining the distribution type for the life model, the very long lives pertaining to the fully automated SAW test specimen (Series 1b) are excluded from the present data base. These specimens had a peculiar shape of the weld toe and very long lives. The reason for excluding these results is that we shall focus on the results at the left tail of the fitted life distribution models. Hence, abnormal long lives on the right tail are not of interest. Our selected data population will consequently be representative for manual and semi-manual welding procedures. The SAW specimens are outliers in this respect. In the present work the following types of probability distributions were fitted to the collected data sample:

- The 2-parameter log-normal distribution
- The 2-parameter Weibull distribution
- The 3-parameter Weibull distribution

Results from the present analysis and the fitted distributions are illustrated in Fig. 5.

Only the 2-parameter log-normal distribution and the 3-parameter Weibull distribution passed the chi-square goodness-of-fit test at a 5% significance level. The log-normal distribution gave a better fit than 3-parameter Weibull distribution. Furthermore, as can be seen from Fig. 5, the log-normal distribution gives a better fit at the left tail where the safe life limit is determined. The main conclusion to be drawn from the present descriptive statistical analysis is that the 2-parameter log-normal distribution applied in rules and regulations is an appropriate choice for characterizing the life model for the collected life data. The competing model based on the 2-parameter Weibull model did not pass the chi-square test. Furthermore, the 3-parameter Weibull distribution gave a poorer fit to the data than the log-normal distribution,

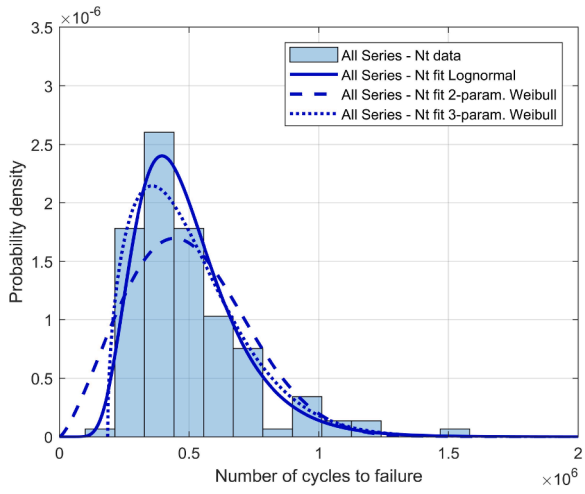

Fig. 5. Fitted probability distributions (128 samples, SAW excluded).

particularly to the important left tail of the distribution. The failure rate functions pertaining to the various distributions are shown in Fig. 6. As can be seen the Weibull model is highest in the very beginning before the log-normal failure rate increases and passes. However, the failure rate function for the log-normal model levels off when the median value for the life has been passed. This difference is generally not emphasized in engineering but gives important information for welded details in aging structures.

As conclusive remark it should be added that the model is validated at a stress range of 150 MPa and it may not represent the correct model for substantial lower stress ranges.

5. Resistance curves obtained by the RFLM

5.1. Analysis of CA fatigue lives

In the present section the RFLM methodology described in Section 3 is applied to establish fatigue resistance curves under CA loading. For the present analyses a large portion of data (216 samples) were collected at various stress ranges, particularly at lower stress ranges [42–47]. Some of these data are runouts such that the conventional linear regression analysis is not capable of including them. An RFLM analysis is carried out and the results are shown in Fig. 7. The three curves in Fig. 7 are 1) the rule-based curve, 2) the conventional S-N curves for the present data and 3) the RFLM resistance curve for the present data. The rule-based curve designated F class and is equal to the 71 category and is based on a larger amount of data. A resume of the model parameters is given in Table 6. As can be seen from the numbers in Table 6, the difference between the present conventional curve and the curves

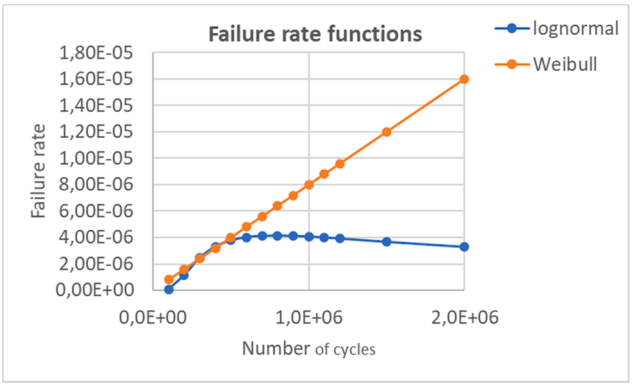

Fig. 6. Failure rate function of the Weibull and lognormal life models.

pertaining to the F class is benign and is owed to the fact that the present data is limited compared to the huge database pertaining to the curves in rules and regulations. On this background we shall emphasize the differences found between the present conventional S-N curve and the RFLM curve as they are both based on the same collected data. But it should be commented that the all the three mean curves in Fig. 7 do coincide when the number of cycles is below 2×10^6. The design curves defined at a 97.5% probability of survival are also quite close in the same area. The small differences in these curves are caused by a small difference in the scatter of the applied data. As can be seen from Fig. 7 the present conventional mean curve and the RFLM mean curve are parallel at about 3×10^5 cycles. The discrepancy in the upper left region of the diagram is caused by the lack of data for the RFLM in this high stress regime. More data could be provided to force the RFLM curve to become almost linear in this area, but this area is not the primary stress range area of the present investigation. Above the given parallel point at 3×10^5 cycles, the conventional straight line will be accepted. The design curves in Fig. 7 are somewhat more separated than the mean curves in the same stress cycle region. However, the curves are not very different before 10^6 cycles are passed. If we focus on fatigue lives longer than 10^6 cycles it is interesting to compare the stress ranges for the two curves at 2×10^6 cycles. This is the fatigue life that is used for defining the fatigue strength and the associated fatigue category in Eurocode 3 Part 1-9. Following the procedures described in Section 2, the fatigue strength is 69 MPa for the present conventional curve whereas it is 74 MPa when defined at the RFLM curve. The increase in the fatigue strength found by the RFLM curve is reflecting the optimism inherent in the long-life data and the runouts. This gives a hyperbola curve that has the opposite curvature compared to the hyperbola used in the conventional theory. This optimism is lost when these data are excluded by the conventional analysis. The increase in fatigue strength is close to 7% and the increase in predicted fatigue life will be close to 20% in this stress region. These increases are substantial. In the high cycle regime, it is noticed that the RFLM design line continues to drop between $N = 10^7$ cycles and $N = 10^8$ cycles. This is in contradiction with the assumption of the existence of a fatigue limit in this area. Parameters of the fitted S-N curves and the S-N curves from codes are presented in Table 6. Only parameters that exist in basic equations are listed. The complete set of parameters of the fitted RFLM model is shown in Fig. 7.

Fig. 7 also shows that the RFLM design curve predicts significantly longer lives beyond 2×10^6 cycles before the stress ranges decrease to the conventional fatigue limit of 48 MPa defined at 5×10^6 cycles according to Eurocode 3 Part 1-9 for detail category 71. The RFLM curve crosses this conventional horizontal fatigue limit line at about 2×10^7 cycles. Beyond this life the RFLM model will in fact predict shorter fatigue lives than the conventional design curve given by Eurocode 3. This is an important nonconformity when comparing with the conventional curves. If we compare with the conventional design curve where it is assumed that the fatigue limit is given at 10^7 cycles the RFLM curve will predicts longer lives up until 10^9 cycles is reached.

5.2. Defining the RFLM design curve for CA loading

Based on the discussion in Section 5.1, the final CA design curve obtained by the RFLM can be defined. The proposed design curve is shown in Fig. 8 together with the conventional S-N curve obtained from the present data. In the illustration the latter linear curve is chosen to have a fatigue limit at 10^7 cycles and not at 5×10^6 cycles as in Eurocode 3 Part 1-9. The RFLM design curve is defined at 97.5% probability of survival. The obtained resistance curve is accepted as it is; however, to the left of 3×10^5 cycles, the RFLM curve shall be parallel with the conventional linear S-N curve, i.e. $m = 3.0$. The chosen point is where the RFLM curve is close to tangential to the conventional linear curve. The argument for this choice is that there is no reason to question the conventional analysis in this high stress range regime. This part of the conventional S-N curve is in the gravity centre of the data included in the

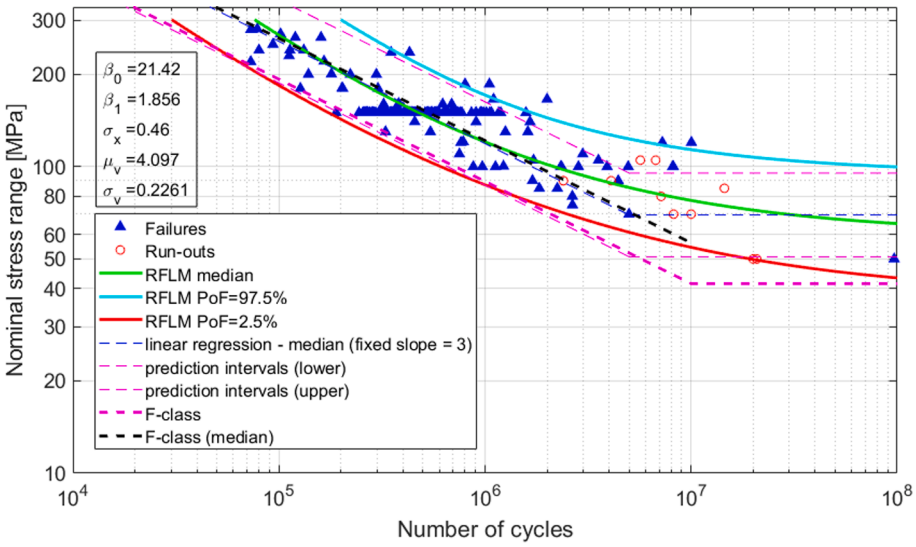

Fig. 7. RFLM fitted to all available data with plate thickness 20–32 mm, (SAW samples excluded).

Table 6
S-N curve parameters.

S-N curve	Mean curve	Design curve
Category 71 (Eurocode 3, part 1-9)	Not given	$\log a_1 = 11.855$ $m_1 = 3$
F-class (DNV)	$\log a_1 = 12.255$ $m_1 = 3$	$\log a_1 = 11.855$ $m_1 = 3$
Conventional S-N curve for the present data	$\log a_1 = 12.227$ $m_1 = 3$	$\log a_1 = 11.817$ $m_1 = 3$
RFLM for the present data	$\beta_0 = 21.42$ $\beta_1 = 1.856$ $\gamma = \exp(\mu_v) = \exp(4.097) = 60.2$	no direct parameters for probabilistic model, can be found by fitting to the numerical results with approximation function of the same type as basic RFLM Eq. (3)

linear regression analysis. The conventional design S-N curve gives a fatigue limit of 40 MPa for the present data. As can be seen from the figure the RFLM curve will predict longer CA lives than the conventional curve between 10^6 cycles and 10^9 cycles. For stresses below the conventional fatigue limit of 40 MPa the RFLM will predict finite long lives beyond 10^9 cycles, but not infinitely long as is the case for the conventional curve predictions.

It is obvious that the non-linear RFLM curve is more in agreement with the lower data points than the conventional S-N curve. But the RFLM curve has increased uncertainty at very low stresses due to the scarcity of data in this long-lasting life area. As shown, the RFLM curve will give more optimistic CA life predictions than the conventional curve if the fatigue limit is defined at 10^7 cycles. However, this is not the case if the conventional fatigue limit had been drawn at 5×10^6 cycles as recommended in Eurocode 3 Part 1-9. The design curve suggested by IIW is also included in Fig. 8. As this curve is keeping $m = 3$ down to the knee point at 10^7 cycles and has a constant slope parameter of $m = 22$ beyond this point, the curve becomes significantly more pessimistic than the present RFLM curve. It must be born in mind that the two curves are not obtained from the same data sample.

6. Considerations for the underlying damage mechanisms

As discussed in Section 2.5 the chosen probabilistic models and the

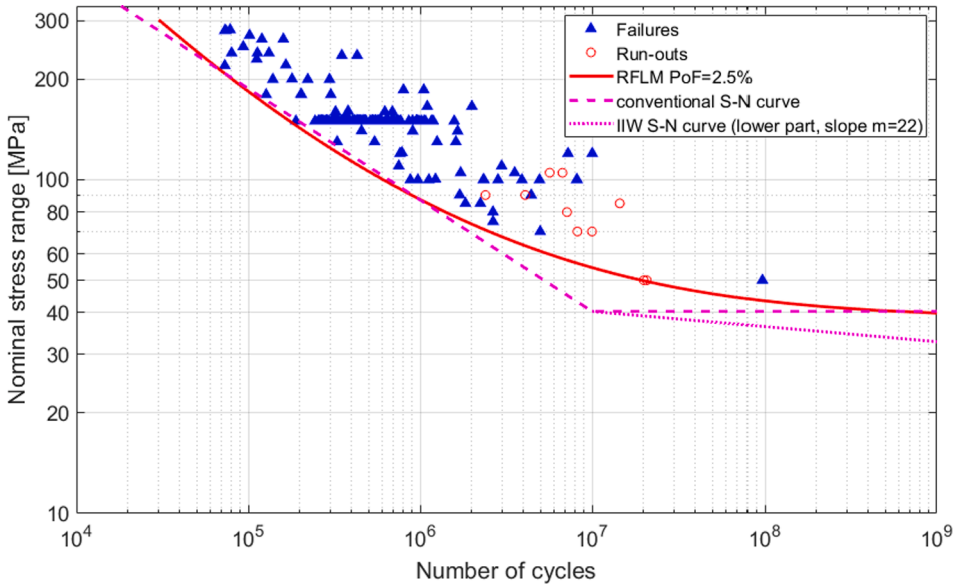

Fig. 8. Design S-N curves based on RFLM for CA loading together with the conventional S-N curve.

involved damage fatigue mechanisms shall be compatible. For the high stress ranges the present analysis confirms what is accepted as common knowledge, the upper linear S-N curve has a slope parameter m that coincides with the exponent m in the Paris crack propagation law:

$$\frac{da}{dN} = C(\Delta K)^m for \Delta K \geq \Delta K_0 \tag{7a}$$

$$\frac{da}{dN} = 0 for \Delta K < \Delta K_0 \tag{7b}$$

Hence, the fatigue life in this area consists mainly of crack growth as described by Eq. (7a). The RFLM curve continues to fall at lower stress ranges, but the slope of the curve gets more and more shallow. However, the RFLM curve does not turn into a horizontal line. This observation does in fact reject the hypothesis that a fatigue limit exists. The traditional explanation for such a fatigue limit has been that the stress intensity factor range ΔK for a given initial cracklike defect is less than the threshold value ΔK_0, i.e. as explained by Eq. (7b). Variations of such models have been used by Haibach [48] and Gurney [49,50] to establish S-N curves both for CA and VA loading. This results in an abrupt knee-point of the conventional S-N curve. In the present work the shape of the lower part of the RFLM curve demonstrates that the fatigue damage mechanism is changing gradually from crack growth to a crack initiation mechanism such that the crack initiation phase becomes the dominant part of the fatigue life. It is the present authors opinion that this shift in damage mechanisms is a better description of the physical realities than a cut-off given by the threshold value based on LEFM and Eq. (7b). To investigate this topic further the RFLM curve is split into two parts. One part is defined by a crack growth mechanism only. The corresponding curve is obtained by extrapolating the upper linear curve with slope parameter m down to a low stress range level of 1 MPa. When subtracting this crack growth life curve from the total RFLM curve given in Fig. 8 the other phase of the damage mechanism is obtained. The result is shown in Fig. 9. A conspicuous finding is that the curve obtained by subtracting the crack growth is also very close to being a straight line for a log-log scale. This curve agrees with common mechanic models for time to crack initiation such as the Coffin-Manson equation. If the present curve is linearized between 10^7 and 10^8 cycles the slope parameter m is close to $m_2 = 10$. This is in good agreement with the inverse value of the fatigue strength exponent ($-1/b$) of the elastic part of the Coffin-Manson equation. The equation can be written:

$$\frac{\Delta\sigma}{2} = \sigma_f^{'}(2N_i)^b \tag{8}$$

where $\Delta\sigma$ is now the weld notch stress range, $2N_i$ is the number of reversals to crack initiation, $\sigma_f^{'}$ is the fatigue strength coefficient and b is the fatigue strength exponent. The equation can be written:

$$N_i = \frac{1}{2}\frac{\left(2\sigma_f^{'}\right)^{-1/b}}{(\Delta\sigma)^{-1/b}} \tag{9}$$

The notch stress range $\Delta\sigma$ at the weld toe is directly linear proportional to the nominal stress S under linear elastic conditions. This is assumed to be the case when the number of cycles to failure is longer than 10^7 cycles. The mean stress effect can be modelled by adding the Morrow correction to Eq. (9):

$$N_i = \frac{1}{2}\frac{\left(2\left(\sigma_f^{'} - \sigma_m\right)\right)^{-1/b}}{(\Delta\sigma)^{-1/b}} \tag{10}$$

where σ_m is the local mean stress at the weld toe notch. The formula allows to take into account the magnitude of the residual stresses.

It should be added that the random variations in the strength exponent b can be substantial such that other results for the second slope parameter of the S-N curve are possible. Baptista et al. [31], found a value close to 12, and even the slope parameter of 22 suggested by Sonsino [15] cannot be completely rejected. However, Sonsino did not consider the possibility that the slope of the S-N curve may change gradually beyond 10^6 cycles. One should also be aware of that if the Coffin-Manson equation is adopted as the governing equation in this low stress regime it will lead to different slopes of the S-N curves for various steel grades. High strength steels will have the shallowest slope, i.e. the highest parameter m. This is well known for welded joints that have been subjected to post weld improvement techniques. However, the phenomenon is usually neglected for as-welded joints. The present discussion is summarized in Table 7. The low cycle fatigue phenomenon with number of cycles to failure less than 10^4 cycles is not included. These short lives are not within the scope of the present study. In the medium cycle area with lives between 10^4 and 10^6 cycles both the mechanical models pertaining to the S-N curve and the RFLM curve is given by the Paris propagation law. In the high cycle area where N is between 10^6 and 10^7 cycles the S-N curve is still assuming that the Paris propagation law alone is governing the damage evolution, but now a possible cut-off given by the threshold value for the SIFR is included. In this stress region the RFLM curve is supported by a two-phase model where both the time to crack initiation and the time spent in crack growth play an important role.

The model for the conventional S-N curve that ignores the crack initiation phase will result in an S-N curve that gives overly pessimistic life predictions in this curve segment. Finally, in the very high cycle regime with $N > 10^7$ cycles, the S-N curve will predict infinite lives supported by the threshold value for the SIFR, whereas the RFLM will predict very long lives with the same two-phase model as before. The only difference for the underlying physical model for the RFLM curve is that the initiation part of the fatigue life has become dominant. It is the authors opinion that the LEFM applied to explain the fatigue endurance limit given by the S-N curves should be rejected. Extensive testing has shown that there exists a significant initiation period in the fatigue lives even at stress levels as high as 150 MPa and with lives less than 10^6 cycles (Mikulski and Lassen [20,21]). The test series in this work had an initiation period close to 20% of the total fatigue life when defined as the time to reach a crack depth of 0.1 mm. This becomes even more pronounced at stress ranges giving fatigue lives beyond 10^7 cycles. The life data from the test series were typical for an F class detail such that the fatigue quality of the joint is representative for this category. The same investigation also demonstrated that the involved welding imperfections do not have a size large enough such that LEFM can be directly applied from the very beginning of the damage process such as assumed when constructing the conventional S-N curves. An objection to the present underlying physical model for the RFLM curve is that it does not

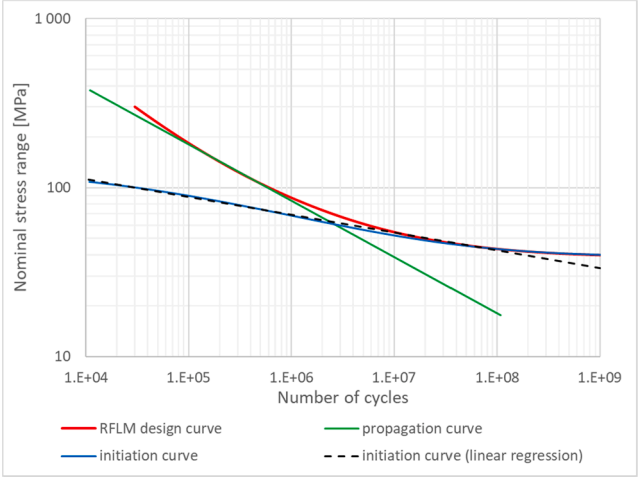

Fig. 9. Splitting the RFLM design curve into two straight lines for crack initiation and crack growth.

Table 7
The reciprocal relation between the probabilistic model and the mechanical models.

Fatigue type categorization	Damage mechanisms	Segment of conventional S-N curve	Basic physical equation S-N curve	Segment of RFLM resistance curve	Basic physical equation RFLM
medium cycle fatigue 10^4–10^6cycles	mainly crack growth	upper straight line	Paris law	upper straight line	Paris law
high cycle fatigue 10^6–10^7cycles	crack initiation and crack growth	lower part of straight line	Paris law	transition segment with maximum curvature	Coffin- Manson equation and Paris law
very high cycle fatigue longer than 10^7 cycles	mainly crack initiation	lower horizontal line from knee point	threshold cut-off in Paris law	lower segment which approaches a straight line	Coffin-Manson equation

explicitly model the influence of weld imperfections such as micro defects and non-metallic inclusions. A good review of possible weld imperfections is given by Hobbacher [14]. Hence, our model does not include possible micro crack nucleation, subsequent crack growth and possible crack arrest. Zerbst et al. [51] have modelled such micro crack behavior in welded joints and LEFM is not applicable. In the present case these topics would have given a physical three-phase model which also could have agreed with the shape of the RFLM resistance curve. However, the present authors have been reluctant to include this third phase, as the underlying model would become more complicated. It is our opinion that the present two-phase model strikes the balance between accuracy in life prediction and model simplicity. The possible weakness is that the initiation life model is developed for a theoretical microstructure without weld imperfections such as small defects. However, the crack initiation curve is in the present case obtained directly from experimental life data by subtracting the crack growth phase, such that any initial defects or flaws are indirectly accounted for in the initiation model. Consequently, the parameters in the physical model will reflect the presence of such possible flaws although the theoretical model was originally developed for a flawless microstructure.

7. Discussion and conclusions

The results from descriptive statistical analysis and probabilistic modelling for the fatigue life in fillet welded steel joints subjected to CA loading have been presented. The plate thicknesses are ranging from 20 to 32 mm and the steel qualities are mild and medium strength C-Mn steel. The welded details are originally designated category 71 in Eurocode 3 Part 1-9, whereas same population is designated as an F class in offshore rules and regulations. Various elementary life models at a given stress range are studied and the construction of conventional S-N curves is included. Finally, the more advanced resistance curves obtained by the RFLM are fitted to the test data. The results from the various models are compared and discussed. Based on the obtained results the following conclusions can be drawn:

1) For the fatigue life data collected at a constant stress range of 150 MPa it is demonstrated that the two-parameter log-normal distribution gives the best fit to the test results. The Weibull distribution gives a poorer fit to the life histogram. This finding supports the common life model applied for the S-N curves in current rules and regulations where the underlying linear regression analysis implies a normal distribution for a log-log scale.
2) The acceptance of the log-normal distribution for the fatigue life gives more optimistic safe life predictions than a Weibull distribution does. Furthermore, the log-normal distribution gives a failure rate function that will decay after the mean time to failure (MTTF) has been reached. This is not the case for a Weibull model that gives a steadily increasing failure rate function. The shape of the log-normal failure rate function indicates that when a welded joint has survived many cycles, it has proven its fatigue quality and may continue to be fit for purpose. This is interesting information for aging structures that have passed their fatigue design lives. If the structure has been kept in service by a scheduled program with frequent detailed inspections up to the MTTF one does not necessarily have to increase the inspection frequency during a further life prolongation. However, the decrease in the failure rate function should not be used as an argument for omitting in-service scheduled fatigue inspection for such structures.
3) More life data were collected for the actual detail at various stress ranges to establish S-N curves. The conventional linear regression analysis was carried out using the lower prediction bound as basis for defining the design curves at chosen probability of survival. A comparison between the design curves given by the building codes for civil engineering (e.g. Eurocode 3 Part 1-9) and the codes for marine structures (e.g. DNVGL-RP-C203) was performed. Although somewhat different statistical analysis procedures are applied in the two codes, no significant differences were found in the obtained design curves. The lower prediction bound defined by a 95% probability of survival is recommended when defining the design curve in Eurocode 3 Part 1-9. If the statistical procedure accounts for the hyperbola shape of the prediction interval, this will give the same design curve as the one obtained when the probability of survival is set to 97.5% with the hyperbola shape neglected. The latter procedure is the basis for DNV recommendations. Both procedures give the same design curve.
4) At lower stress levels the linear regression has the unfortunate limitation that it excludes the long-life failures and the runout results. These data are essentially important in the way that they usually are closer to the magnitude of the acting stress ranges in-service than the finite life data entering the linear regression analysis. The short-comings of the conventional S-N curves were eliminated by using the Random Fatigue Limit Model.
5) The design curve obtained by the RFLM is non-linear for a log-log scale. The RFLM design curve is defined at a 97.5% probability of survival. The obtained resistance curve is accepted as it is; however, to the left of 3×10^5 cycles, the RFLM curve shall be parallel with the conventional linear S-N curve. The chosen point is where the RFLM curve is close to tangential to the conventional linear curve. The RFLM fatigue resistance curve will as a result coincide with the conventional linear S-N curve in the medium cycle fatigue range for stress ranges above 80 MPa. Both curves have a slope parameter $m = 3$. This part of the curve is the area where the gravity centre of the test data is found. At lower stresses where the conventional S-N curve has a knee point, the non-linear RFLM curve has its maximum curvature. This shape gives far better agreement with the long-life data in this area. Below the conventional S-N knee point the RFLM curve continues to fall with an increasing slope parameter m with a decreasing curvature. The curve becomes almost linear when 10^7 cycles are passed, but the curve does not become horizontal.
6) When comparing with a conventional S-N curve that has a CA fatigue limit at 10^7 cycles, the RFLM curve is very close to tangential to both the upper line segment and the fatigue limit when approaching 10^8 cycles. Consequently, the RFLM curve will

almost always give more optimistic CA life predictions compared to predictions based on the conventional curves found for offshore structures.

7) When comparing with a conventional S-N curve that has a CA fatigue limit at 5×10^6 cycles (as the category 71 in Eurocode 3 Part 1-9 for civil engineering), the RFLM curve is still very close to tangential to the upper line segment, but the RFLM curve has a more pessimistic shape compared to the conventional fatigue limit. For a large band of stress ranges the RFLM curve will in fact predict shorter fatigue lives than the conventional curve.
8) The comparison with the conventional curves from the offshore industry and Eurocode 3 Part 1-9 indicates that a fatigue limit drawn at 10^7 cycles is a better choice than drawing it at 5×10^6 cycles for a detail category 71. However, the RFLM resistance curve does in fact reject the existence of a fatigue limit before 10^9 cycles is reached. This rejection agrees well with the latest proposal for CA S-N curves from IIW. However, the IIW curve predicts significantly shorter fatigue lives close to its knee-point. There is still a lack of data in this very high cycle regime to support a final conclusion on this matter.
9) Based on the above observations the present RFLM resistance curve is not envisioned to replace the conventional S-N curves found in rules and regulations. However, the RFLM curve gives an important supplement for fatigue assessment in the high cycle regime.
10) It has been demonstrated that the shape of the obtained RFLM resistance curve agrees well with a two-phase model for the involved damage mechanisms. An initiation model based on the Coffin-Manson equation and a crack growth model based on the Paris propagation law have been proposed. These models will support the RFLM resistance curve to handle changes in important variables such as the applied stress ratio and the magnitude of the residual stresses.
11) Future work will be focusing on how to handle VA loading with the present RFLM resistance curves. The split into two separate curves and the conclusion drawn in clause 9) above will play an important role in this work. The support from the underlying physical equations is expected to increase the accuracy of the calculated damage accumulation. This will be the hypothesis for the future work.

Declaration of Competing Interest

The authors declare that they have no known competing financial interests or personal relationships that could have appeared to influence the work reported in this paper.

Acknowledgements

The authors would like to thank their colleagues within the Technical Committee 6 for Fatigue in the European Convention for Constructional Steelwork (ECCS) for valuable criticism and comments during the work carried out for the completion of the present paper. This work is part of the on-going activities within SFI Offshore Mechatronics project founded by The Research Council of Norway, project number 237896.

Appendix A. Summary of the mathematics for an elementary life model

The probability of failure pertaining to the SLL on the left tail in Fig. 2 in the main text is theoretically obtained by the equation:

$$P(\boldsymbol{t} \le t) = F(t) = \int_0^t f(t')\mathrm{d}t' \tag{A1}$$

The reliability $R(t)$ is defined by the probability of surviving the SLL which is the complementary probability to the expression in Eq. (A1):

$$P(\boldsymbol{t} > t) = R(t|\mu, \sigma, S|\,) \tag{A2}$$

The failure rate function is defined by, Lewis [52]:

$$\lambda(t) = \frac{f(t)}{R(t)} \tag{A3}$$

The failure rate function is a conditional probability function. It gives the probability of failure per time unit just after the time t is reached, given that the joint has survived up to the time t.

Appendix B. Summary of the mathematics for the RFLM curves

With Eq. (3) in the main text as basis, it is assumed that $v = \ln(\gamma)$ has a Probability Density Function (PDF) given by:

$$f_V(v) = \frac{1}{\sigma_v}\varphi_V\left(\frac{v-\mu_v}{\sigma_v}\right) \tag{B1}$$

with location parameter and scale parameter μ_v and σ_v, respectively. $\phi_V(\cdot)$ is the normal frequency function. Let $x = \ln(\Delta S)$ and $W = \ln(N)$. Assuming that V is given and that $V < x$, $W|V$ then has a frequency function:

$$f_{W|V}(w) = \frac{1}{\sigma_x}\varphi_{W|V}\left(\frac{w-[\beta_0 - \beta_1 \ln(\exp(x) - \exp(v))]}{\sigma_x}\right) \tag{B2}$$

with the location parameter $\beta_0 - \beta_1 \ln(\exp(x) - \exp(v))$ and scale parameter σ_x. The marginal frequency function of W is given by:

$$f_W(w) = \int_{-\infty}^{x} \frac{1}{\sigma_x \sigma_v}\varphi_{W|V}\left(\frac{w-[\beta_0 - \beta_1 \ln(\exp(x) - \exp(v))]}{\sigma_x}\right)\varphi_V\left(\frac{v-\mu_v}{\sigma_v}\right)dv \tag{B3}$$

The marginal Cumulative Distribution Function (CDF) of W is given by:

$$F(w) = \int_{-\infty}^{x} \frac{1}{\sigma_v} \Phi_{W|V}\left(\frac{w - [\beta_0 - \beta_1 \ln(\exp(x) - \exp(v))]}{\sigma_x}\right) \varphi_V\left(\frac{v - \mu_v}{\sigma_v}\right) dv \quad \text{(B4)}$$

where $\Phi_{W|V}(\cdot)$ is the CDF of W|V. Further details are found in [32,33].

Appendix C. Life data for the Drebenstedt and Euler example

Life data from [28,29]

Stress range [MPa]	Cycles	failure/runout
265	42,000	failure
265	70,000	failure
265	79,000	failure
202	107,000	failure
202	188,000	failure
202	204,000	failure
139	537,000	failure
139	597,000	failure
108	800,000	failure
108	1,077,000	failure
108	5,000,000	runout
108	5,200,000	runout
108	5,400,000	runout
74	5,000,000	runout
74	5,200,000	runout

Appendix D. Life data at a stress range of 150 MPa

Series 1a		Series 1b		Series 2		Series 3		Series 4	
A3	387,235	A11	999,119	S2-1	323,520	S3-1	326,810	B2	1,578,652
A4	370,248	A15	603,314	S2-2	262,950	S3-2	551,000	B3	636,004
A5	436,426	A23	523,562	S2-3	259,310	S3-3	552,900	B5	599,388
A6	483,540	A27	523,656	S2-4	270,510	S3-4	416,860	B6	571,395
A8	647,939	A28	505,000	S2-5	454,300	S3-5	632,400	B7	376,006
A9	544,635	A31	1,490,400	S2-6	265,970	S3-6	1,073,630	B8	658,011
A10	336,070	A35	2,073,554	S2-7	314,480	S3-7	707,270	B9	410,012
A12	576,732	A40	651,503	S2-8	323,290	S3-8	387,380	B10	446,519
A13	428,970	A43	1,074,052	S2-9	286,650	S3-9	370,620	B11	590,574
A14	374,064	A48	1,008,050	S2-10	189,270	S3-10	1,016,410	B12	318,504
A16	512,159			S2-11	305,120	S3-11	859,160		
A17	424,542			S2-12	282,630	S3-12	679,950		
A18	334,876			S2-13	283,220	S3-13	650,260		
A20	588,573			S2-14	388,710	S3-14	984,700		
A21	414,214			S2-15	330,070	S3-15	771,560		
A22	352,006			S2-16	312,400	S3-16	522,390		
A24	553,546			S2-17	244,490	S3-17	729,880		
A25	478,004			S2-18	327,230	S3-18	582,590		
A29	702,468			S2-19	294,680	S3-19	705,180		
A30	594,047			S2-20	255,400	S3-20	905,440		
A33	456,790			S2-21	367,388	S3-21	432,050		
A34	361,002			S2-22	390,560	S3-22	647,280		
A36	551,015			S2-23	472,230	S3-23	954,790		
A37	527,270			S2-24	305,266	S3-24	484,140		
A38	332,513			S2-25	425,700	S3-25	693,870		
A39	734,505			S2-26	376,390	S3-26	379,470		
A41	525,507			S2-27	268,250	S3-27	1,163,580		
A42	349,059			S2-28	404,030	S3-28	549,230		
A44	580,007			S2-29	276,320	S3-29	522,380		
A45	382,012			S2-30	319,820	S3-30	323,960		
A46	447,015			S2-31	374,080	S3-31	1,191,670		
A47	445,007			S2-32	310,590	S3-32	565,680		
A49	465,717			S2-33	362,750	S3-33	947,660		
A50	345,074			S2-34	356,300	S3-34	455,550		
				S2-35	326,170	S3-35	463,760		
				S2-36	367,110	S3-36	530,000		
				S2-37	365,450	S3-37	736,780		
				S2-38	288,810	S3-38	527,320		
				S2-39	380,690	S3-39	754,890		
				S2-40	334,540	S3-40	532,700		
				S2-41	346,350	S3-41	901,850		
				S2-42	366,210	S3-42	713,450		

References

[1] Murakami Y, Takagi T, Wada K, Matsunaga H. Essential structure of S-N curve: Prediction of fatigue life and fatigue limit of defective materials and nature of scatter. Int J Fatigue 2021; 146. doi:10.1016/j.ijfatigue.2020.106138.
[2] Hobbacher A. Recommendations for Fatigue Design of Welded Joints and Components. Springer; 2016. doi:10.1007/978-3-319-23757-2.
[3] Radaj D, Sonsino CM, Fricke W. Fatigue Assessment of Welded Joints by Local Approaches. Elsevier Science; 2006.
[4] Lassen T, Recho N. FLAWS Fatigue Life Analyses of Welded Structures. ISTE 2006.
[5] Lotsberg I. Fatigue Design of Marine Structures. Cambridge: Cambridge University Press; 2016. doi:10.1017/CBO9781316343982.
[6] Maddox SJ. Fatigue Strength of Welded Structures (Second Edition). Second Edi. Woodhead Publishing; 1991. doi:10.1016/B978-1-85573-013-7.50002-1.
[7] EN 1993-1-9:2005. Eurocode 3: Design of steel structures - Part 1-9: Fatigue; 2005.
[8] HSE. Offshore rules; 1991.
[9] DNVGL. DNVGL-RP-C203: Fatigue Design of Offshore Steel Structures; 2016.
[10] ABS. Guide for Fatigue Assessment of Offshore Structures. Standardization 2003; 2014:1–56.
[11] ISO 12107:2012. Metallic materials — Fatigue testing — Statistical planning and analysis of data; 2012.
[12] ECCS Technical Committee 6 - Fatigue. Background Documentation 9.01a: Background information on fatigue design rules – Statistical evaluation – 3rd Draft; 2018.
[13] Schijve J. Fatigue Predictions and Scatter. Fatigue Fract Eng Mater Struct 1994;17: 381–96. https://doi.org/10.1111/j.1460-2695.1994.tb00239.x.
[14] Hobbacher AF. The new IIW recommendations for fatigue assessment of welded joints and components - A comprehensive code recently updated. Int J Fatigue 2009;31:50–8. https://doi.org/10.1016/j.ijfatigue.2008.04.002.
[15] Sonsino CM. Course of SN-curves especially in the high-cycle fatigue regime with regard to component design and safety. Int J Fatigue 2007;29:2246–58. https://doi.org/10.1016/j.ijfatigue.2006.11.015.
[16] Wirsching PH. Report no. 17: The statistical distribution of cycles to failure. Paramus, NY: 1984.
[17] Engesvik K, Moan T. Probabilistic analysis of the uncertainty in the fatigue capacity of welded joints. Eng Fract Mech 1983;18:743–62. https://doi.org/10.1016/0013-7944(83)90122-4.
[18] ENV 1993-1-1: 1992, Eurocode 3: Design of steel structures; 1992.
[19] DNV. Recommended practice RP-C203: Fatigue Strength Ananlysis of Offshore Steel Structures; 2001.
[20] Mikulski Z, Lassen T. Fatigue crack initiation and subsequent crack growth in fillet welded steel joints. Int J Fatigue 2019;120:303–18. https://doi.org/10.1016/j.ijfatigue.2018.11.014.
[21] Mikulski Z, Lassen T. Crack growth in fillet welded steel joints subjected to membrane and bending loading modes. Eng Fract Mech 2020;235:107190. https://doi.org/10.1016/j.engfracmech.2020.107190.
[22] Lassen T, Recho N. Proposal for a more accurate physically based S-N curve for welded steel joints. Int J Fatigue 2009;31:70–8. https://doi.org/10.1016/j.ijfatigue.2008.03.032.
[23] Benjamin JR, Cornell CA. Probability, Statistics, and Decision for Civil Engineers. McGraw-Hill; 1970.
[24] Bastenaire FA. New Method for the Statistical Evaluation of Constant Stress Amplitude Fatigue-Test Results. In: Heller RA, editor. Probabilistic Asp. Fatigue, West Conshohocken, PA: ASTM International; 1972, p. 3–28. doi:10.1520/STP35402S.
[25] Hobbacher A. Fatigue Design of Welded Joints and Components. Woodhead Publishing; 1996. doi:10.1533/9780857093189.34.
[26] Hobbacher A. Recommendations for fatigue design of welded joints and components. Doc. XIII-1251-07, XV-1254-07. 2007.
[27] Cooper BE. Statistics for Experimentalists. Oxford: Pergamon Press; 1969.
[28] Euler M, Kuhlmann U. Statistical intervals for evaluation of test data according to Eurocode 3 Part 1-9. ECCS Technical committee 6 - Fatigue, Contribution to working group 6.3 Statistical analysis of fatigue data; 2013.
[29] Drebenstedt K, Euler M. Statistical Analysis of Fatigue Test Data according to Eurocode 3. In: Powers, Frangopol, Al-Mahaidi, Caprani, editors. Maintenance, Safety, Risk, Manag. Life-Cycle Perform. Bridg., London: Taylor & Francis Group; 2018, p. 2244–51.
[30] Schneider CRA, Maddox SJ. Best practice guide on statistical analysis of fatigue data; 2003.
[31] Baptista C, Reis A, Nussbaumer A. Probabilistic S-N curves for constant and variable amplitude. Int J Fatigue 2017;101:312–27. https://doi.org/10.1016/j.ijfatigue.2017.01.022.
[32] Pascual FG, Meeker WQ. Estimating fatigue curves with the random fatigue-limit model. Technometrics 1999;41:277–89. https://doi.org/10.1080/00401706.1999.10485925.
[33] Lassen T, Darcis P, Recho N. Fatigue Behavior of Welded Joints Part 1 - Statistical Methods for Fatigue Life Prediction. Weld J 2005;84:183s–7s.
[34] D'Angelo L, Nussbaumer A. Estimation of fatigue S-N curves of welded joints using advanced probabilistic approach. Int J Fatigue 2017;97:98–113. https://doi.org/10.1016/j.ijfatigue.2016.12.032.
[35] Toasa Caiza PD, Ummenhofer T. General probability weighted moments for the three-parameter Weibull Distribution and their application in S-N curves modelling. Int J Fatigue 2011;33:1533–8. https://doi.org/10.1016/j.ijfatigue.2011.06.009.
[36] Toasa Caiza PD, Ummenhofer T. A probabilistic Stüssi function for modelling the S-N curves and its application on specimens made of steel S355J2+N. Int J Fatigue 2018;117:121–34. https://doi.org/10.1016/j.ijfatigue.2018.07.041.
[37] Leonetti D, Maljaars J, Snijder HH (Bert). Fitting fatigue test data with a novel S-N curve using frequentist and Bayesian inference. Int J Fatigue 2017; 105: 128–43. doi:10.1016/j.ijfatigue.2017.08.024.
[38] D'Antuono P. An analytical relation between the Weibull and Basquin laws for smooth and notched specimens and application to constant amplitude fatigue. Fatigue Fract Eng Mater Struct 2020;43:991–1004. https://doi.org/10.1111/ffe.13175.
[39] Lassen T. The effect of the welding process on the fatigue crack growth in welded joints. Weld J 1990; February: 75s-85s.
[40] Engesvik K, Lassen T. The effect of weld geometry on fatigue life. Proc. 7th Int. Conf. Offshore Mech. Arct. Eng. OMAE1988, Houston, Texas: ASME Press; 1988, p. 441–5.
[41] Engesvik K. Analysis of Uncertainties in the Fatigue Capacity of Welded Joints, Report UR-82-17. Trondheim: 1982.
[42] Stötzel J. Collection and evaluation of fatigue test results - RWTH Aachen, ECCS-TC6-Fatigue, IIW-Working Group JWG XIII-XV. n.d.
[43] Lindqvist A, Nilsson H. Effective notch stress analysis of transverse attachments in steel bridges - a parametric fatigue life assessment. Chalmers 2016.
[44] Lebas G, Fauve JC. Collection of fatigue data. Pau: Elf Aquitaine; 1988.
[45] Gurney TR. The Fatigue Strength of Transverse Fillet Welded Joints. Woodhead Publishing; 1991.
[46] Gurney TR. Thickness effect in "relatively thin" welded joints; Offshore Technology Report OTH 91 358; 1995.
[47] Berge S. On the effect of plate thickness in fatigue of welds. Eng Fract Mech 1985; 21:423–35. https://doi.org/10.1016/0013-7944(85)90030-X.
[48] Haibach E. Discussion paper. Weld Inst Conf Fatigue Welded Struct 1970.
[49] Gurney TR. Cumulative damage calcuations taking account of low low stresses in the spectrum. TWI Report 2/1976/E. 1976.
[50] Gurney TR. Cumulative Damage of Welded Joints. Woodhead Publishing; 2006. doi:10.1533/9781845691035.1.
[51] Zerbst U, Madia M, Schork B. Fracture mechanics based determination of the fatigue strength of weldments. Procedia Struct Integr 2016;1:10–7. https://doi.org/10.1016/j.prostr.2016.02.003.
[52] Lewis EE. Introduction to Reliability Engineering. Wiley; 1988.